Monitorización satelital de variables esenciales climáticas: temperatura, salinidad y nivel del mar

Cristina González Haro

Institut de Ciències del Mar (ICM) - Barcelona Expert Center (BEC)

Consejo Superior Investigaciones Científicas (CSIC)

✉ cgharo@icm.csic.es

Copernicus Satellite Data in Chile and Latin America: From applications to networking

BEC
Barcelona Expert Center

22nd March, Valparaíso, Chile

TELE DETECT

THE OCEAN, THE PLANET’S THERMOSTAT

The **ocean** ocean plays a **key role** for the **global climate**:

- stores and distributes large amount of heat around the globe via ocean currents
- **strong heat capacity** (1200 times than atmosphere)
- vertical fluxes of CO_2
- the upper ocean modifies the evolution of troposphere

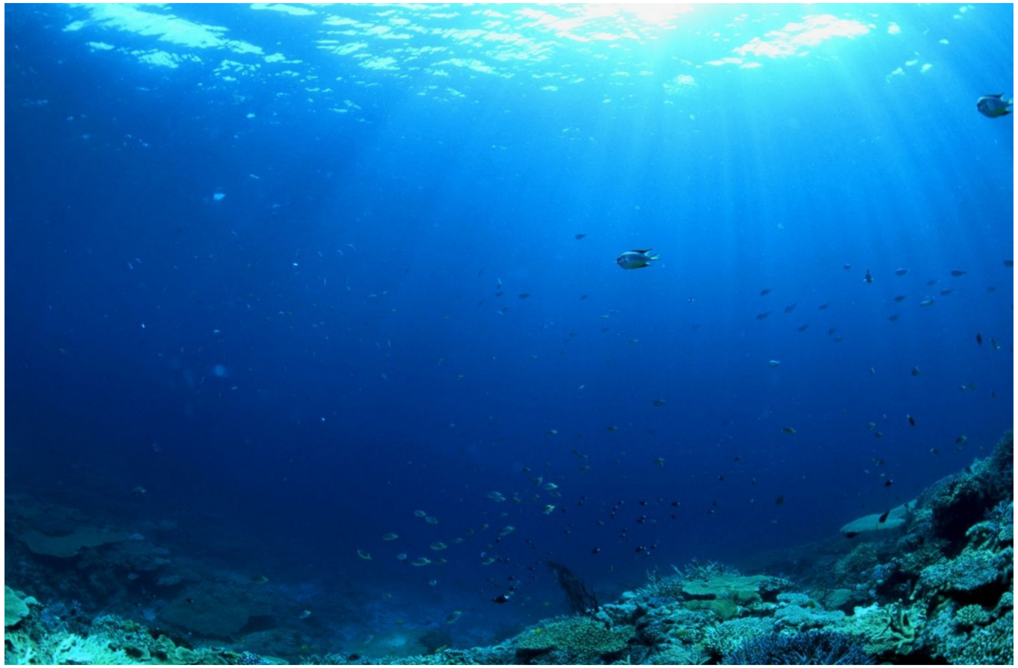

THE OCEAN, THE PLANET'S THERMOSTAT

Ocean currents redistribute the absorbed solar energy. Ocean circulation is controlled by surface winds, by the rotation of the earth and by certain physical properties such as temperature and salinity.

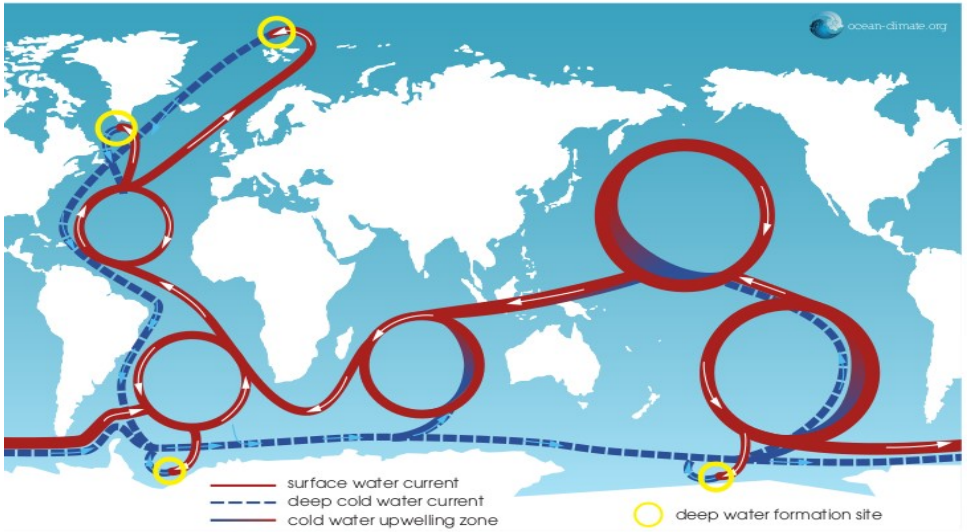

Simplified diagram of the global ocean circulation

ocean-climate.org

3

THE OCEAN, THE PLANET'S THERMOSTAT

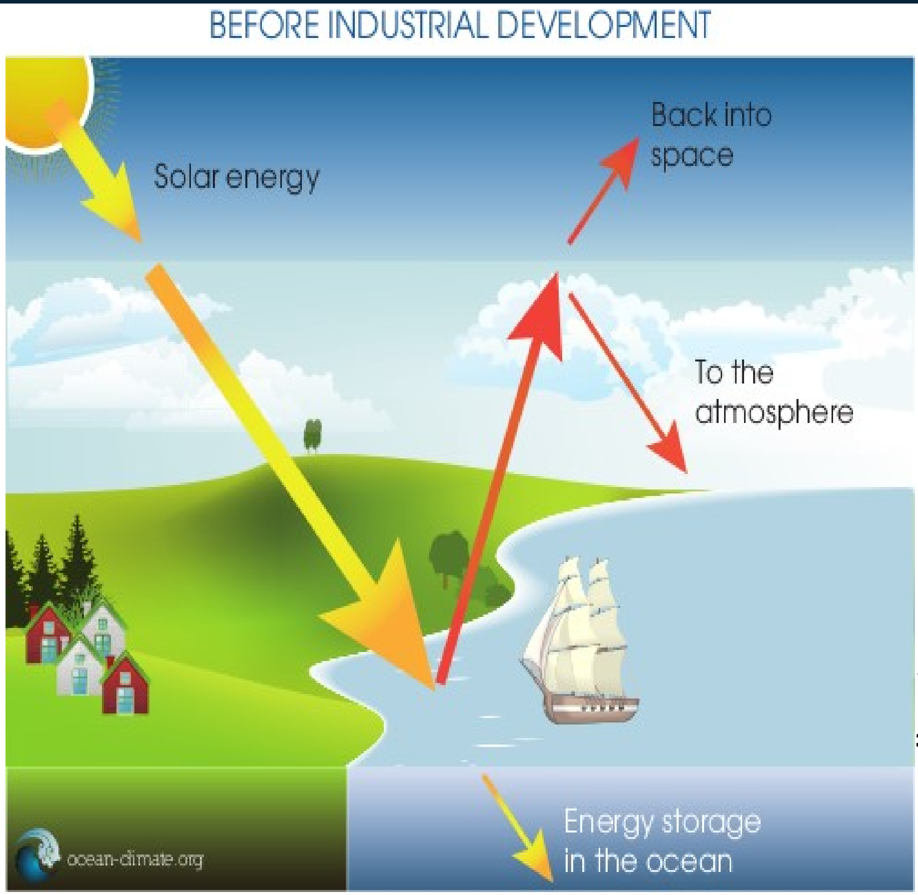

ocean-climate.org

- 93% of the excess heat generated by human activities via the greenhouse effect is absorbed by the ocean, thus mitigating the increase in temperature of the atmosphere.

- The global ocean plays a role in the regulation and control of the large natural planetary balances. It regulates climate fluctuations, that would be much more rapid and more powerful if they were only governed by the atmosphere.

THE OCEAN, THE PLANET'S THERMOSTAT

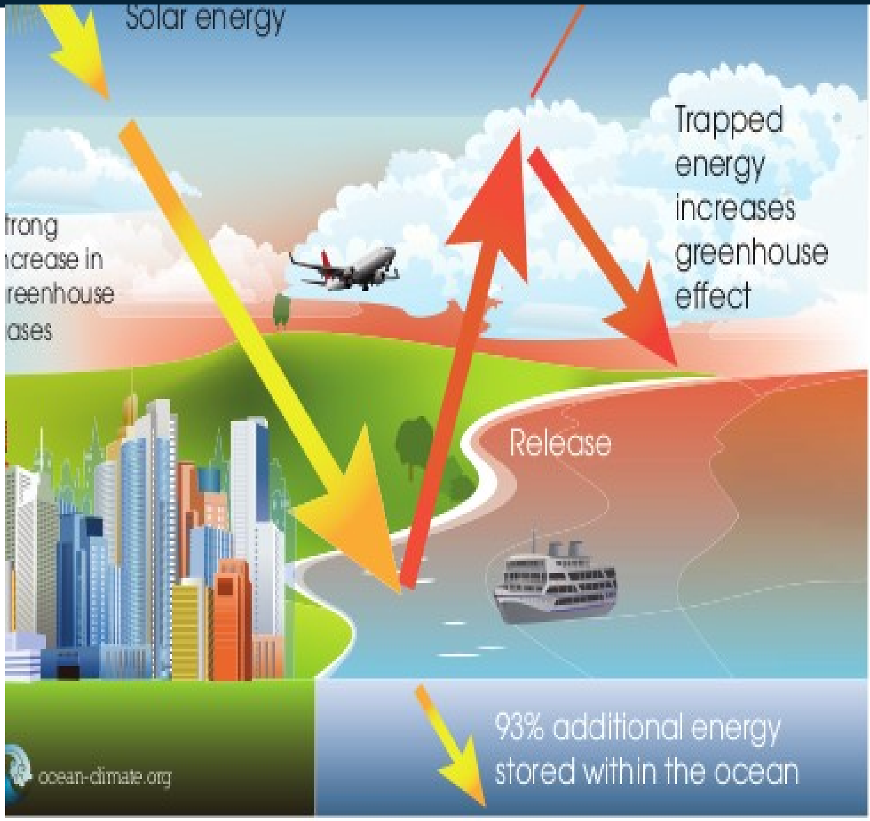

Increase of the greenhouse effect

ocean-climate.org

- 93% of the excess heat generated by human activities via the greenhouse effect is absorbed by the ocean, thus mitigating the increase in temperature of the atmosphere.

- The global ocean plays a role in the regulation and control of the large natural planetary balances. It regulates climate fluctuations, that would be much more rapid and more powerful if they were only governed by the atmosphere.

THE OCEAN, THE PLANET'S THERMOSTAT

BEC
Barcelona Expert Center

- Impact of ocean global warming as seen by satellites

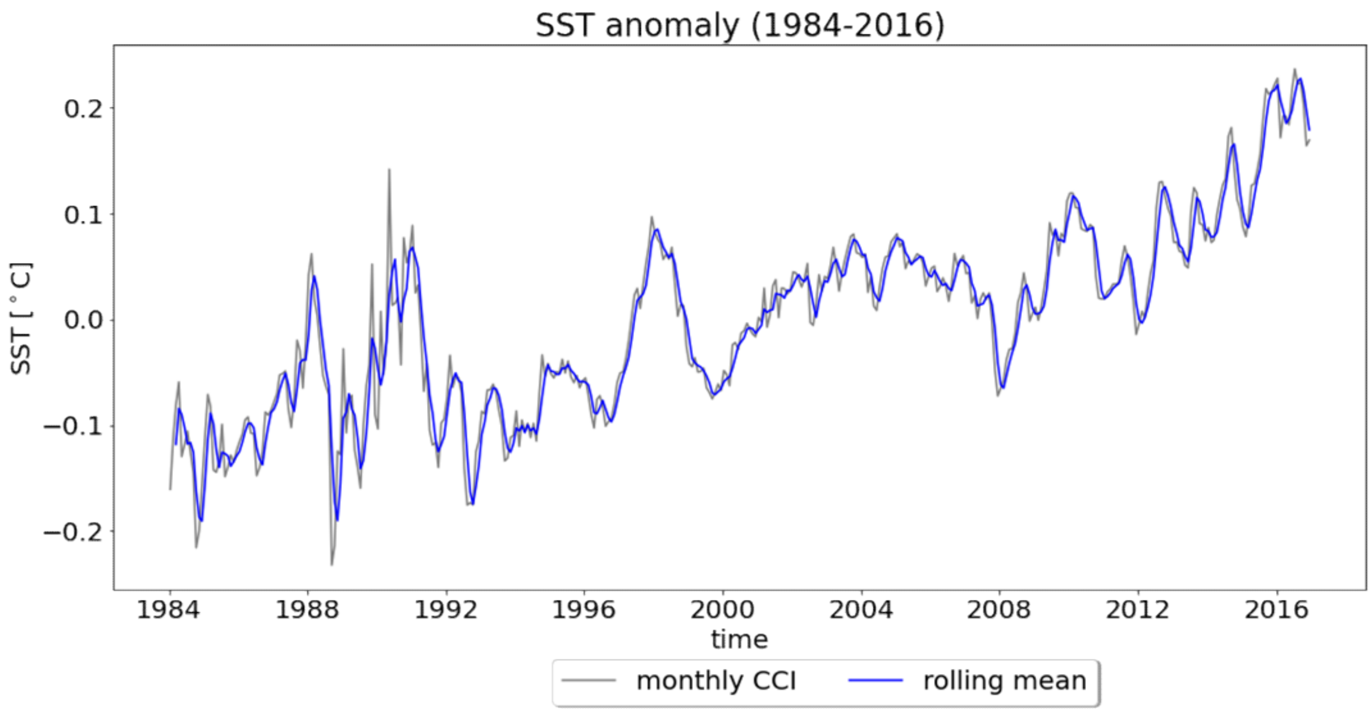

REMOTE SENSING OBSERVABLE PROCESSES

- Electromagnetic (EM) radiation attenuates very fast in the ocean:
  - 80 % of the solar energy is labored in the upper 10 m
  - very little, if any, penetrates below 600m
- Only surface processes can be observed by satellites
  - deep processes with a surface signature
  - acoustic remote sensing

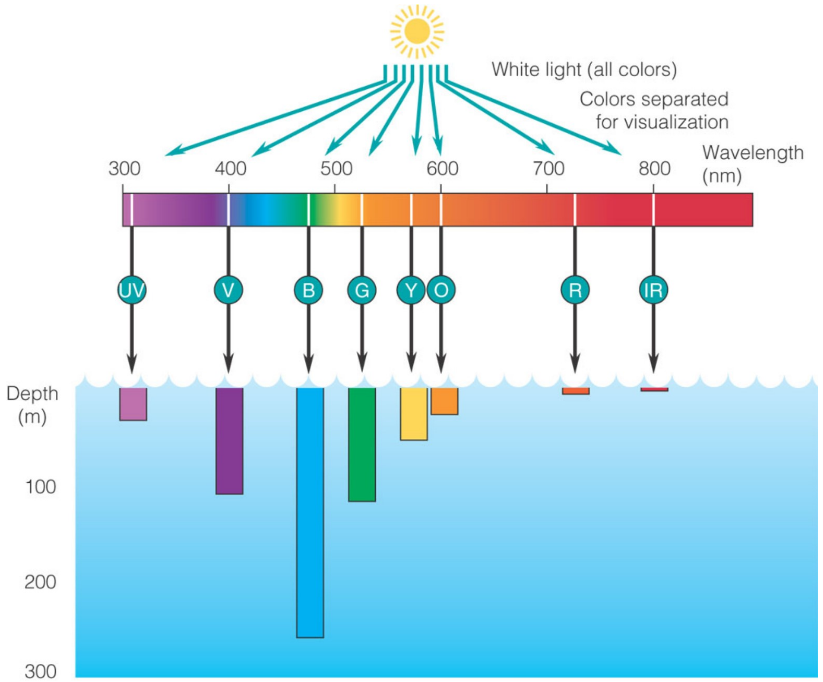

REMOTE SENSING OBSERVABLE PROCESSES

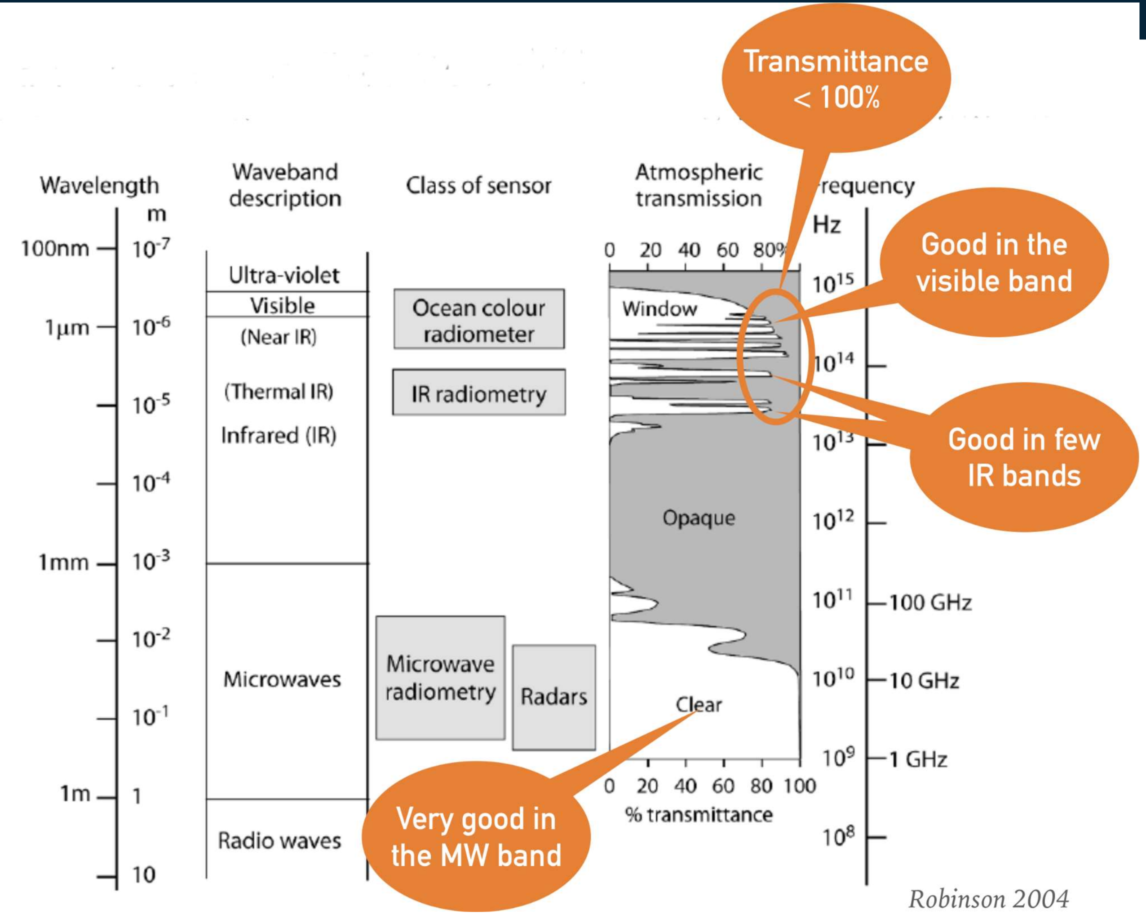

Robinson 2004

REMOTE SENSING OBSERVABLE PROCESSES

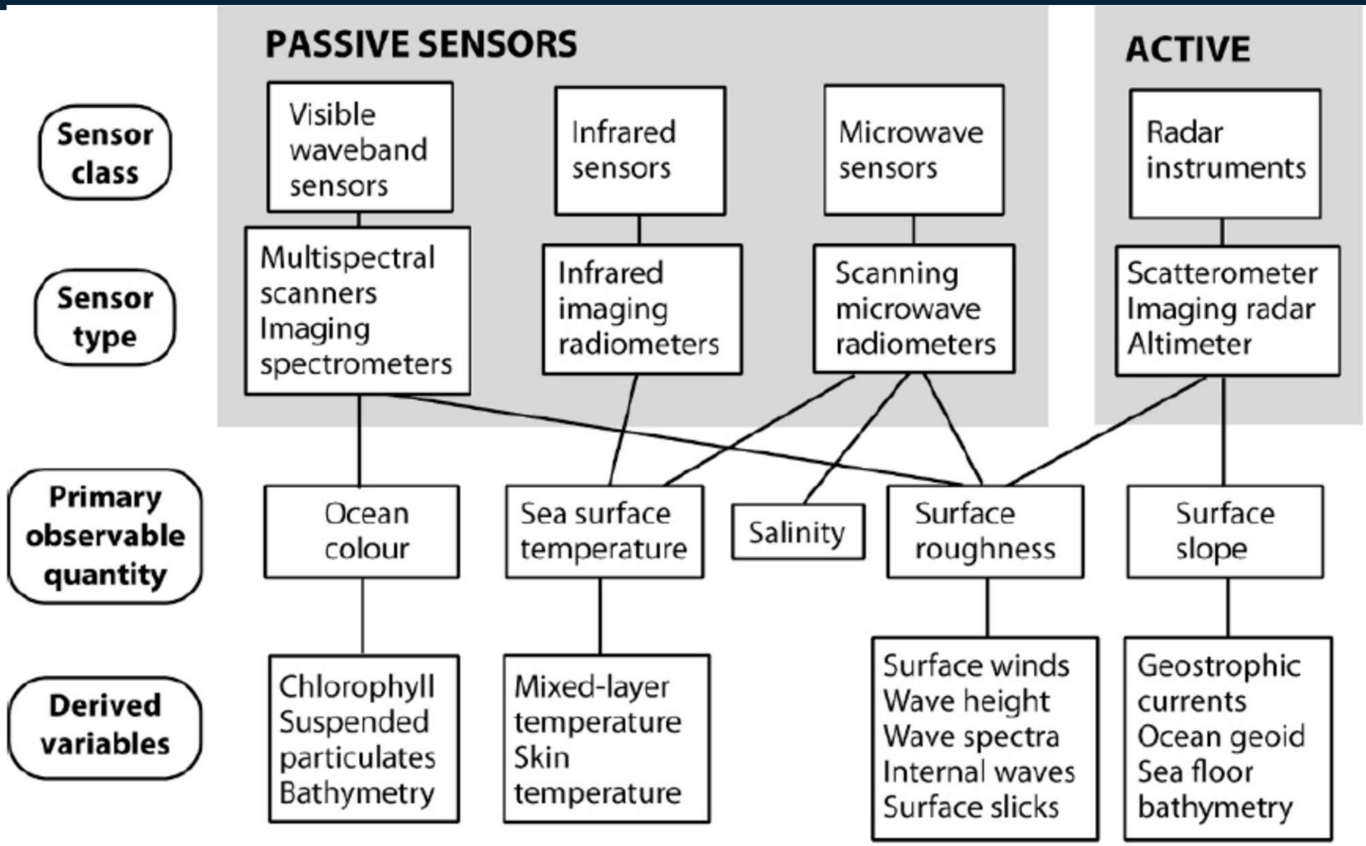

Robinson 2004

REMOTE SENSING OBSERVABLE PROCESSES

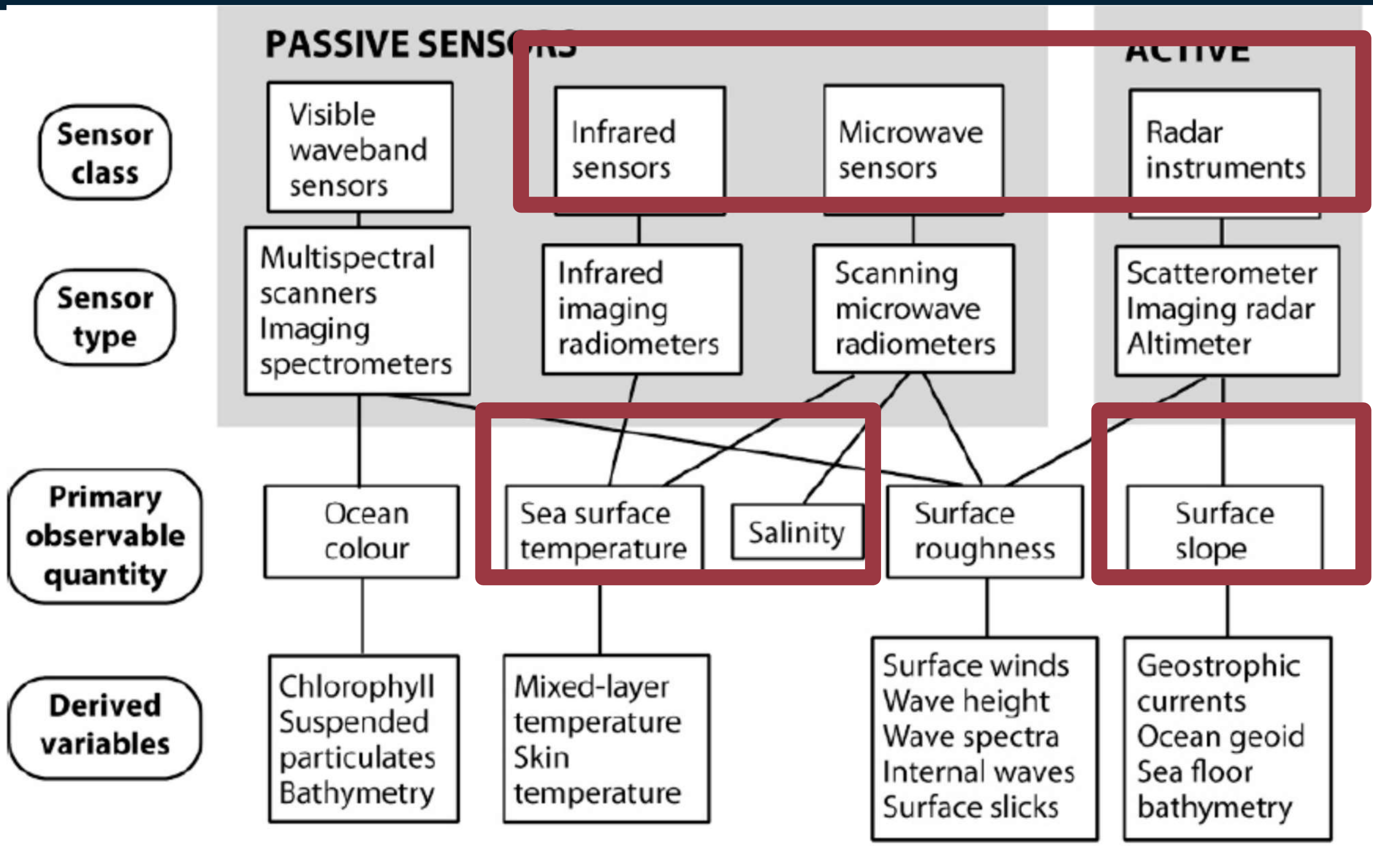

Robinson 2004

REMOTE SENSING OBSERVABLE PROCESSES

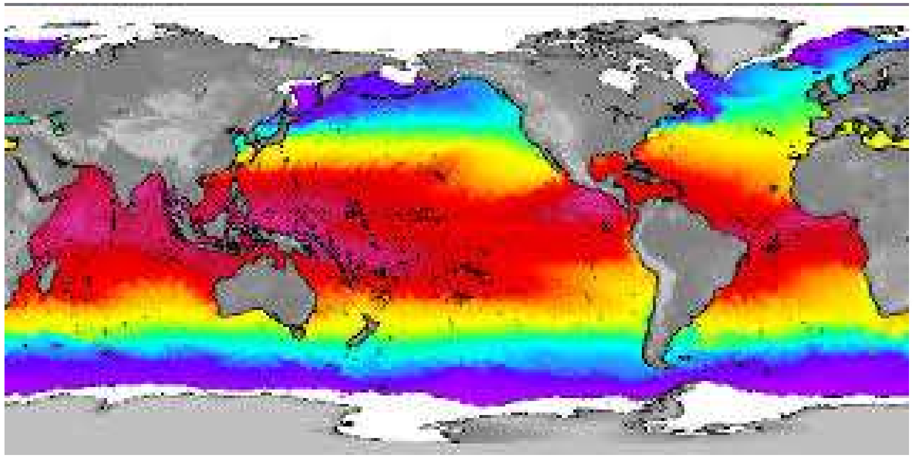

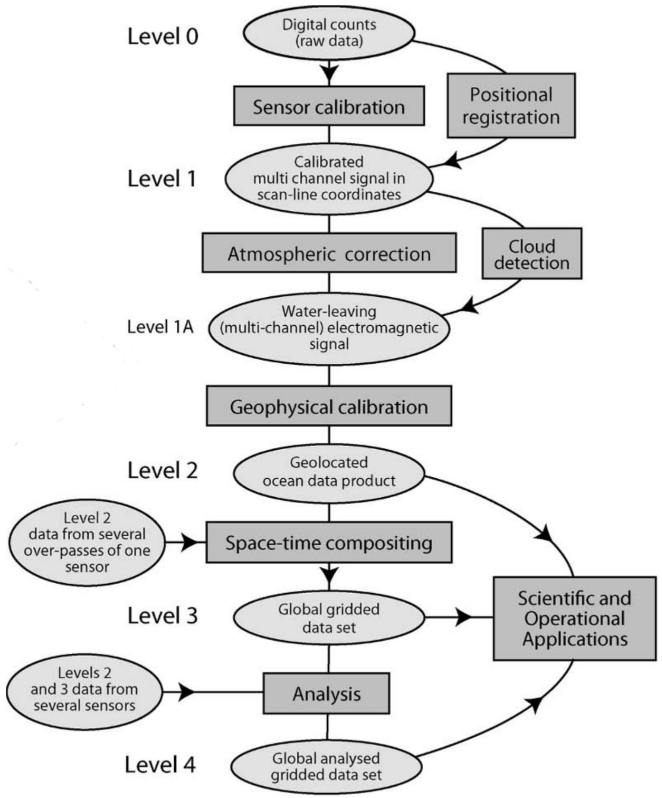

Robinson 2004

REMOTE SENSING OBSERVABLE PROCESSES

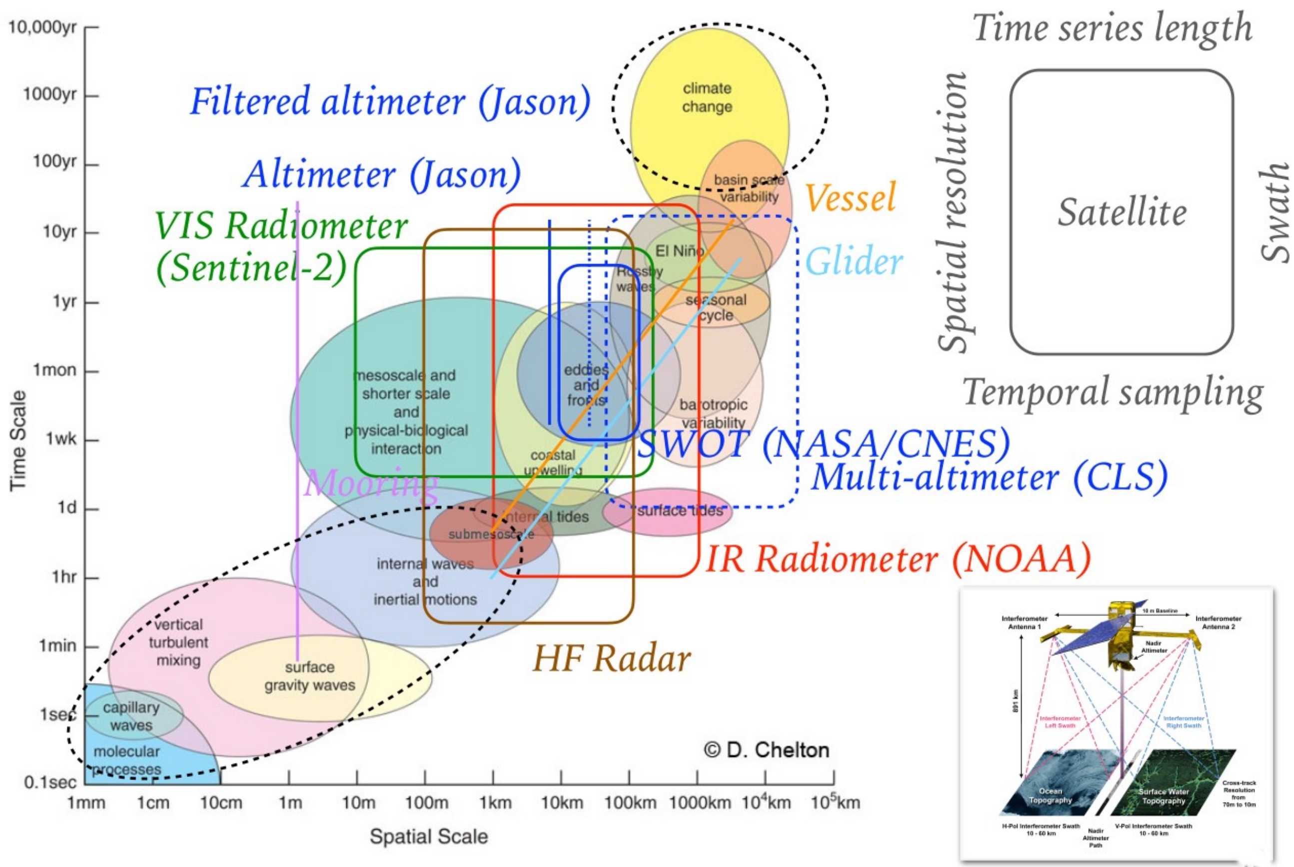

INFRARED RADIOMETERS

- Any body in thermodynamic equilibrium at temperature T radiates energy (Planck's law):

$$M_\lambda(T) = \frac{2hc^2}{\lambda^5} \frac{1}{\exp\left(\frac{hc}{k_B \lambda T}\right) - 1}$$

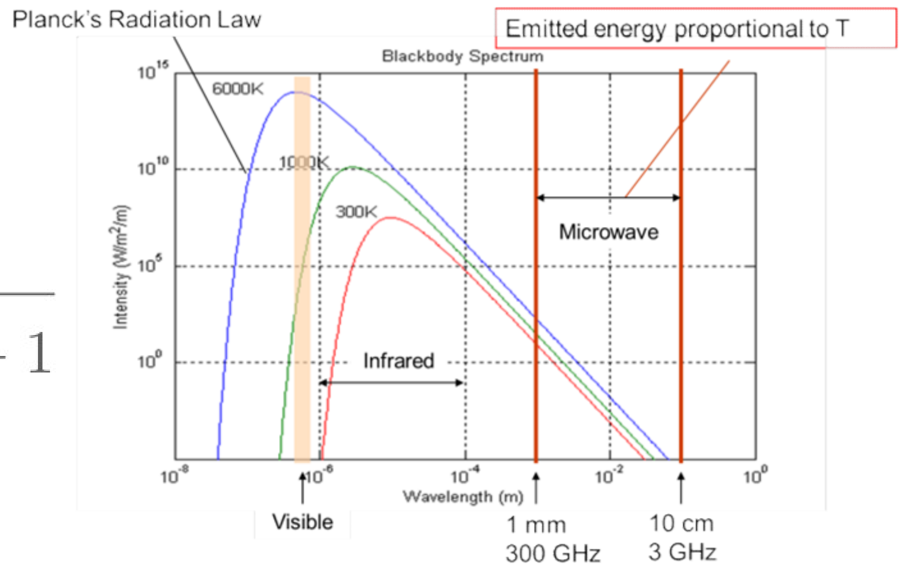

- Radiance measurements allow to estimate the apparent temperature (Brightness Temperature) $L_\lambda = \pi^{-1} M_\lambda$

INFRARED RADIOMETERS

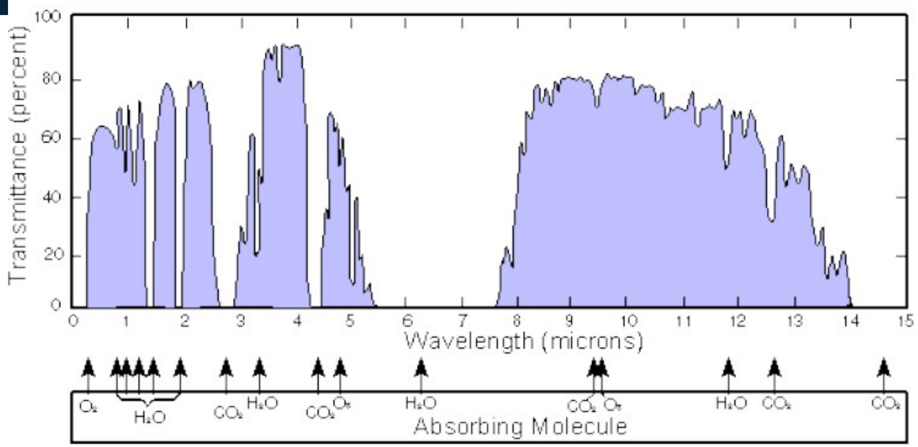

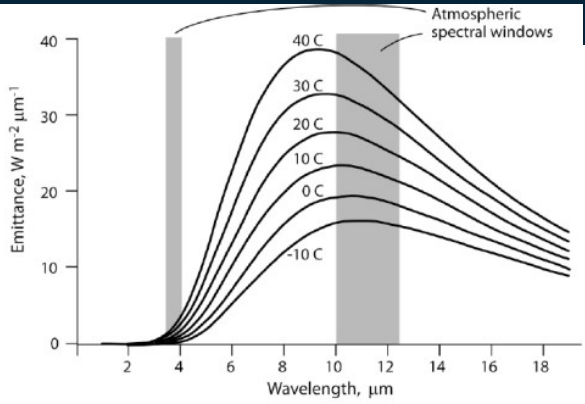

- Transmittance in the IR band (3-14 µm) is not perfect:
  - Only discrete bands are available: 3-4 µm and 9-14 µm
  - Main contribution from H_2O (inhomogeneous), CO_2 and O_3 (homogeneous)
- Atmospheric attenuation reduces Brightness Temperature

INFRARED RADIOMETERS

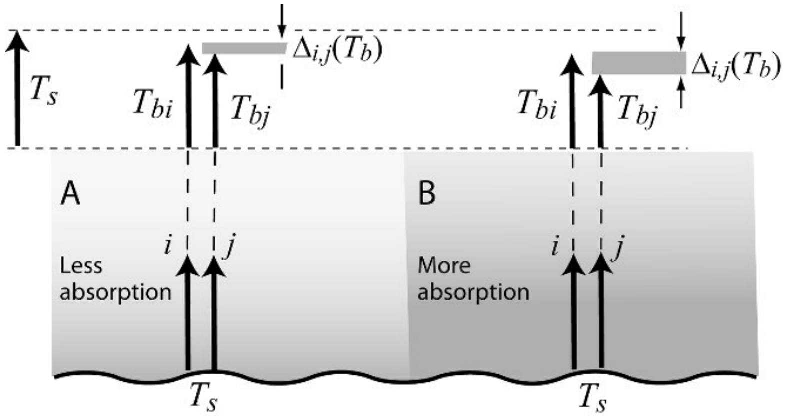

- Attenuation depends on the wavelength
- Use of a multichannel approach to correct for the atmospheric contribution

$$T_s = aT_B(\lambda_1) + b(T_B(\lambda_2) - T_B(\lambda_1)) + c$$

- This is the most extended approach

INFRARED RADIOMETERS

- Alternative approach: observe the ocean from different angles (different atmospheric thickness)

$$T_{ni} \approx T_s - K \sec\theta_n$$

$$T_{fi} \approx T_s - K \sec\theta_f$$

then,

$$T_s = \frac{T_{ni}\sec\theta_n f - T_{fi}\sec\theta_n}{\sec\theta_f \sec\theta_n}$$

- A wise choice of angles (θ_n = 0º, θ_f = 60º) simplifies to:

$$T_s = 2T_{ni} - T_{fi}$$

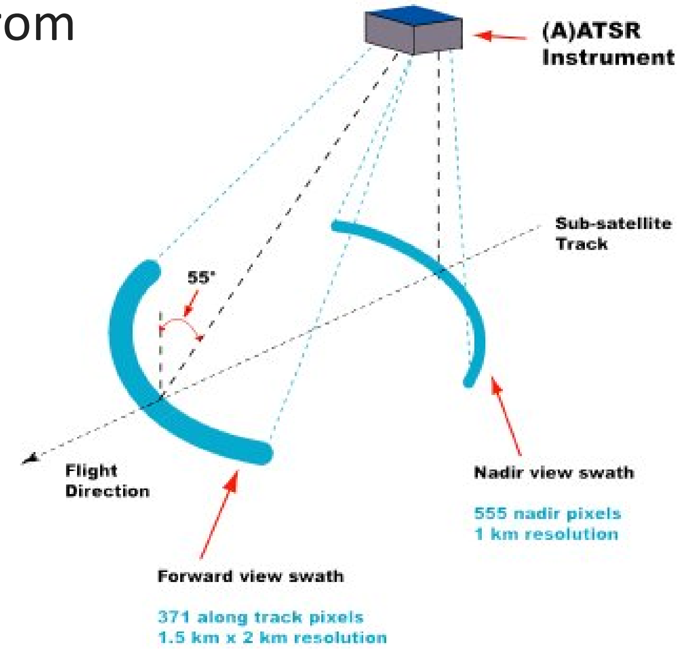

INFRARED RADIOMETERS

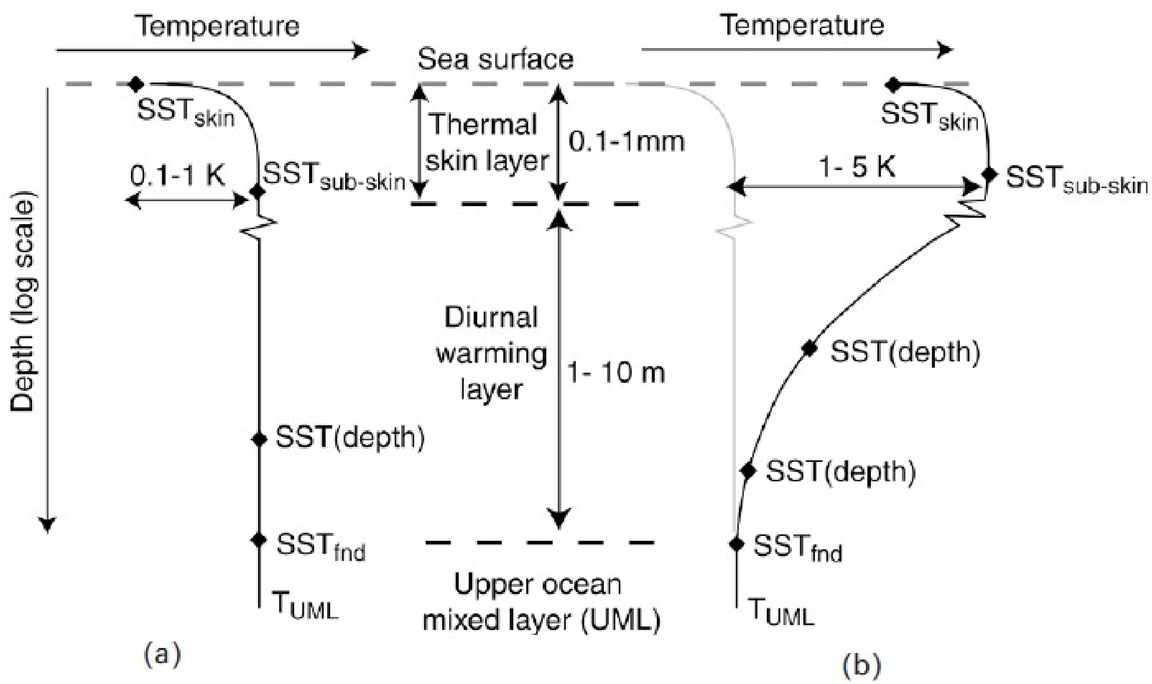

INFRARED RADIOMETERS

BEC
Barcelona Expert Center

Sensor acronym	Platform(s)	Full name of sensor	Agency	Dates (for series)	Main IR spectral bands (μm)
AVHRR/2	NOAA-7, -9, -11, -12, -14	Advanced very high-resolution radiometer, version 2	NASA/NOAA	June 1981- Mar 2001	0.725-1.10 3.55-3.93 10.3-11.3 11.5-12.5
AVHRR/3	NOAA-15, -16, -17, -18, METOP	Advanced very high-resolution radiometer, version 3	NASA/NOAA Eumetsat	May 1998- present	0.725-1.10 1.58-1.64 3.55-3.93 10.3-11.3 11.5-12.5
ATSR-1, ATSR-2, AATSR	ERS-1, ERS-2, Envisat	(Advanced) Along-track scanning radiometer	ESA	Jul 1991- 2000 Apr 1995 - 2011 Sep 2001- 2012	1.45-1.75 3.55-3.85 10.3-11.3 11.5-12.5
MODIS	TERRA, AQUA	Moderate resolution imaging spectrometer	NASA	Feb 2000- present	3.660-3.840 3.929-3.989 4.020-4.080
SEVIRI	Meteosat second generation	Spinning enhanced visible and infrared imager	Eumetsat	Sep 2002- present	1.50-1.78 3.48-4.36 8.30-9.10 9.80-11.80 11.00-13.00
VIIRS	SUOMI NPP	Visible Infrared Imaging Radiometer Suite	NASA	Feb 2011- present	3.660-3.840 3.973-4.128 10.263-11.263
SLSTR	Sentinel-3a Sentinel-3b	Surface Land & Sea Thermal Radimeter	ESA	Feb 2016- present, April 2018-Present	1.45-1.75 3.55-3.85 10.3-11.3 11.5-12.5

MICROWAVE RADIOMETERS

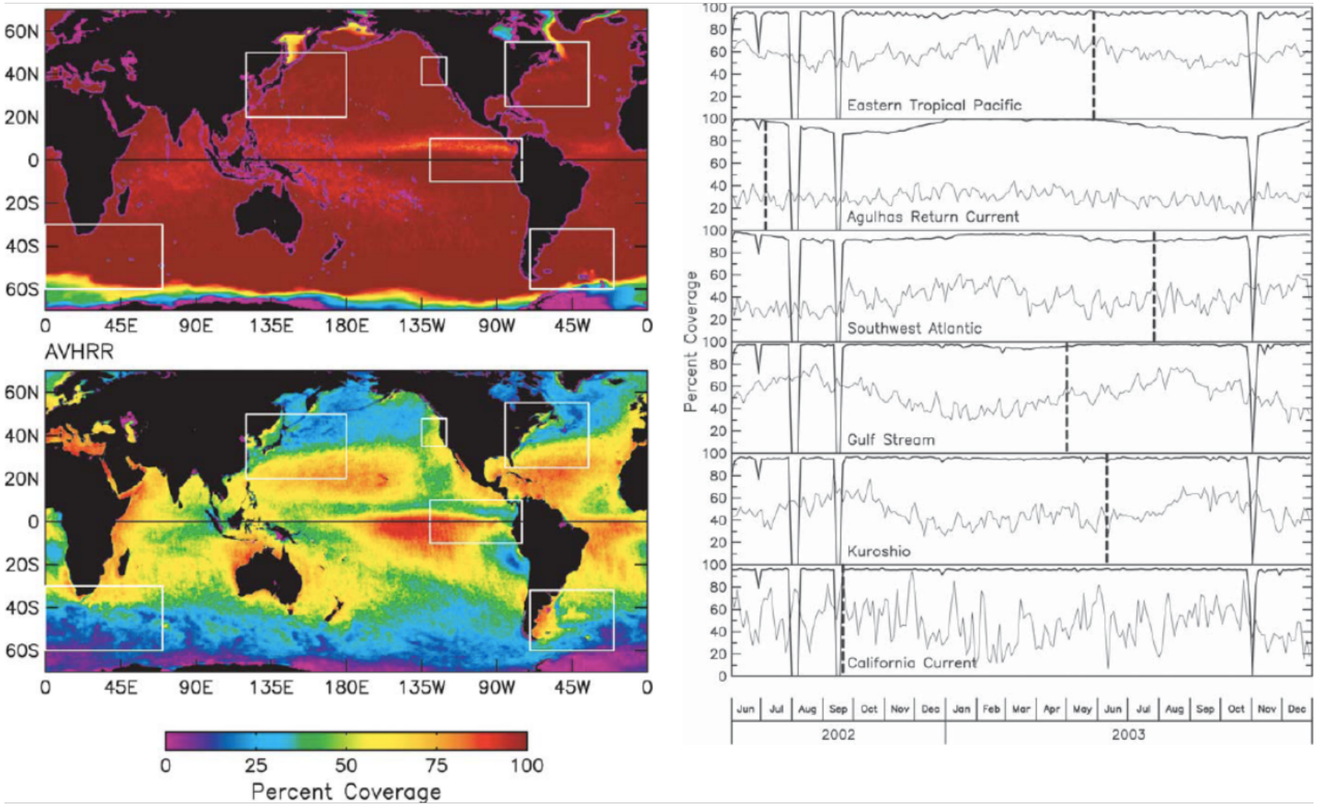

Chelton & Weltz 2005

MICROWAVE RADIOMETERS

BEC Barcelona Expert Center

- Spectral emittance at frequency f emitted by body in thermodynamic equilibrium at temperature T (Planck's law):

$$\hat{B}_f(T) = \frac{2hf^3}{c^2}\frac{1}{\exp\left(\frac{hf}{k_BT}\right)-1}$$

- At microwave range:

$$\exp\left(\frac{hf}{k_BT}\right) \approx 1 + \frac{hf}{k_BT}$$

- Rayleigh-Jeans approximation:

$$\hat{B}_f(T) \approx \frac{2k_Bf^2T}{c^2}$$

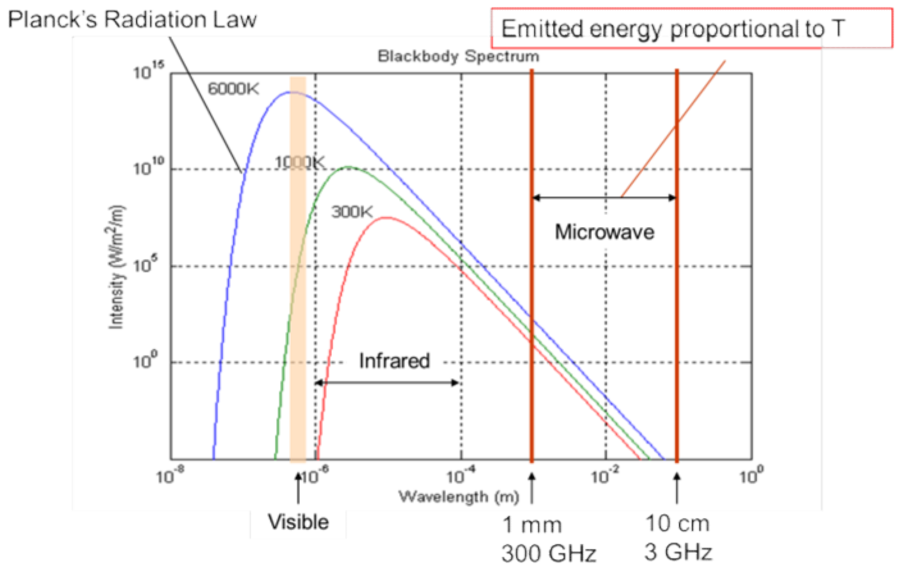

The **emitted radiance** is **directly proportional** to the **temperature** of the emitting surface.

MICROWAVE RADIOMETERS

- Seawater is not a black-body and Planck's law has to be corrected introducing the **emissivity ε**.

$$B_f(T) = \varepsilon \hat{B}_f(T) \approx \varepsilon \frac{2k_B f^2 T}{c^2}$$

- The temperature retrieved without taking into account ε is known as Brightness Temperature T_B
- It is necessary to know the emissivity to retrieve the temperature of the emitter
  - → For infrared radiometry it was not necessary because ε ~ 1
  - → For microwave radiometry ε < 1

MICROWAVE RADIOMETERS

- Emissivity depends on the viewing angle θ, the polarization H, V and the dielectric constant for sea water e(f)

$$\varepsilon_{H,V} = 1 - \rho_{H,V}^2$$

$$\rho_H = \frac{\cos\theta - \sqrt{e - \sin^2\theta}}{\cos\theta + \sqrt{e - \sin^2\theta}}$$

$$\rho_V = \frac{e\cos\theta - \sqrt{e - \sin^2\theta}}{e\cos\theta + \sqrt{e - \sin^2\theta}}$$

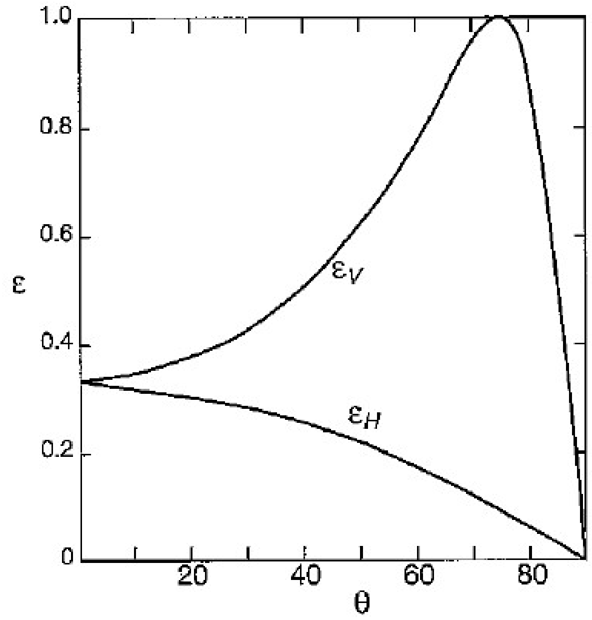

Robinson 2004

MICROWAVE RADIOMETERS

- The roughness of the sea surface creates fluctuations in the incidence angle within the footprint of the radiometer.
  - → Resulting brightness depends on the sea surface slope statistics
  - → Since this is controlled by wind stress, it contains information about winds.
  - → An effective emissivity ε* can be introduced to take roughness into account
- The presence of foam also modifies the emissivity
  - →The presence of foam also depends on wind

- The emissivity not only depends on the viewing angle but also with e

$$e(f) = e_\infty + \frac{e_s - e_\infty}{1 + i2\pi f \tau_r} - i\frac{\sigma}{2\pi f \varepsilon_0}$$

valid for f < 85GHz.

  - → ε_0 is the permittivity of free space
  - → e_∞ is the dielectric constant at very high frequency
  - → e_s is are the dielectric constant at zero frequency
  - → τ_r is the relaxation time
  - → σ is the ionic conductivity

} Depend on T and S

- The consequent dependence of ε on T implies that the relation between microwave brightness and T is not linear.

MICROWAVE RADIOMETERS

- The penetration depth in the microwave range is given by

$$d(f) = \frac{2\pi f \sqrt{e}}{c}$$

  - It depends on T and S
- Penetration depth for IR (λ = 12µm)

  d_{IR} □ 4µm

- Penetration depth for MW (f = 5GHz)

  d_{MW} □ 5mm

- Thickness of the skin-layer

  d_T □ 100µm

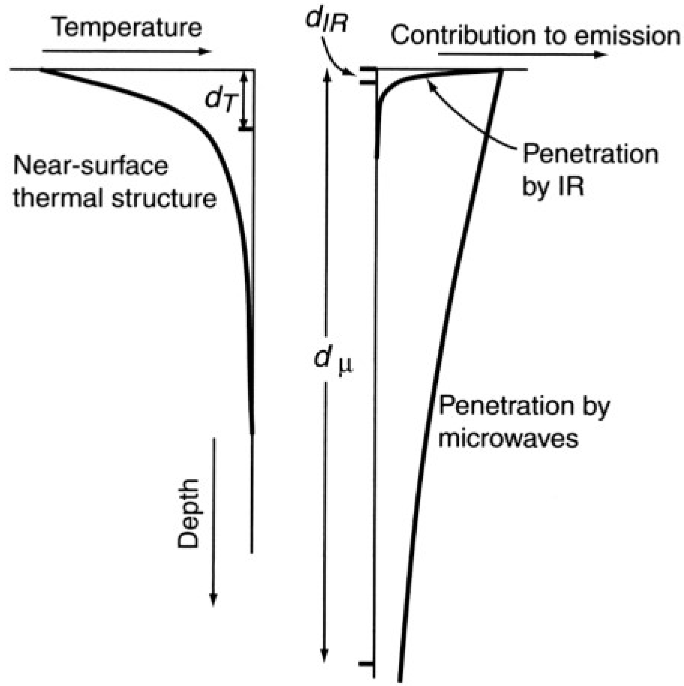

MICROWAVE RADIOMETERS

- The sensitivity of microwave radiance to SST/SSS is necessary to set the mounted channel at the most sensitive frequency
- Maximum sensitivity within the range 4–10 GHz
- The higher frequency channels of microwave radiometers (10 GHz) are less sensitive to SST change in the low SST range

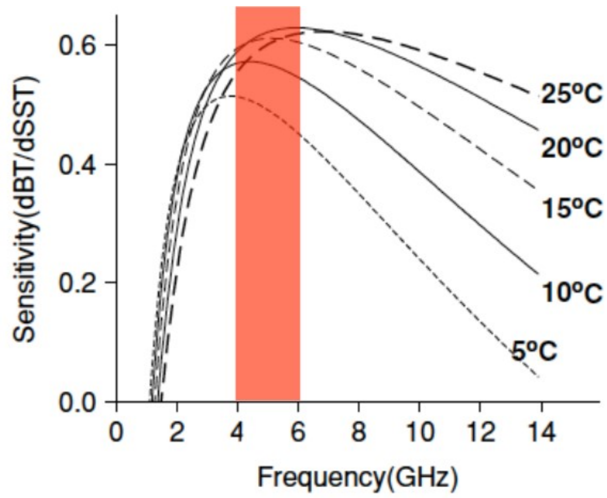

MICROWAVE RADIOMETERS

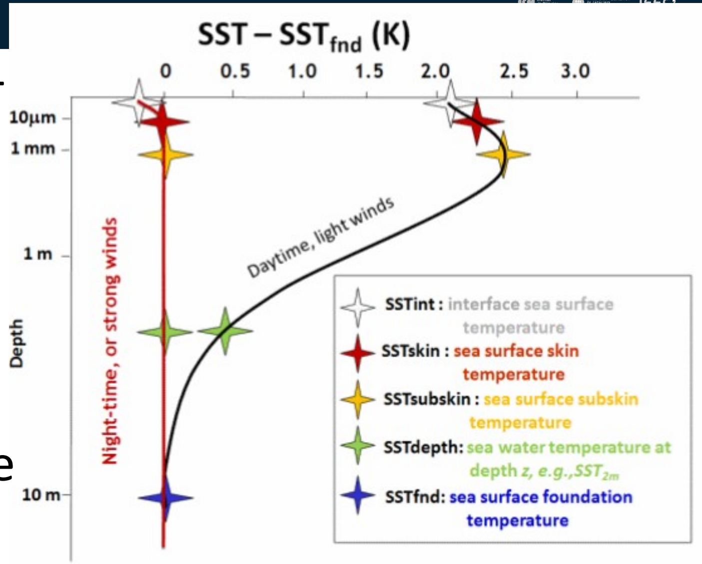

https://www.ghrsst.org/

- SSTint: hypothetical temperature at the exact air-sea interface
- SSTskin: temperature within the conductive diffusion-dominated sub- layer □ 10 – 20µm
  - Measured by an IR radiometer
- SSTsubskin: temperature at the base of the conductive laminar sub-layer of the ocean surface
  - Well approximated to the measurement by a MW radiometer (6-11 GHz)
- SSTdepth: temperature measurements beneath the SSTsubskin
  - Wide variety of platforms and sensors and distinct from those obtained using remote sensing techniques
- SSTfnd: temperature free of diurnal temperature variability

MICROWAVE RADIOMETERS

BEC
Barcelona Expert Center

Radiómetros 1.4GHz

2009	2010	2011	2012	2013	2014	2015	2016	2017	2018	2019	2020	2021	2022	2023	2024	2025	2026	2027

SMOS

Aquarius

SMAP

WCOM

COSM

CIMR

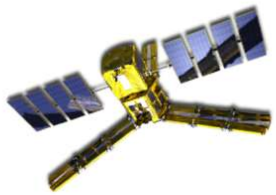

SMOS
Interferometric Radiometer
Spatial res: ~43 km (30-80 km)
Swath: ~1000 km
Global coverage: ~2-3 days
Incidence: 0°- 60°
Full polarization
Launched Nov 2009

Aquarius-SAC/D
Radiometer & scatterometer
Spatial Res: ~100 km
Swath: ~400 km
Global coverage: ~7 days
Incidence angle: 29°,38° & 46°
Full Polarization
Launched Jun 2011

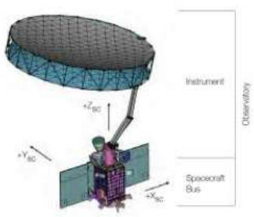

SMAP
Radiometer & SAR
Spatial res: 40 km
Swath: 1000km
Global coverage : ~2-3 days
Incidence angle: 40°
Full Polarization
Launched Jan 2015

BEC
Barcelona Expert Center

Soil Moisture and Ocean Salinity (SMOS)

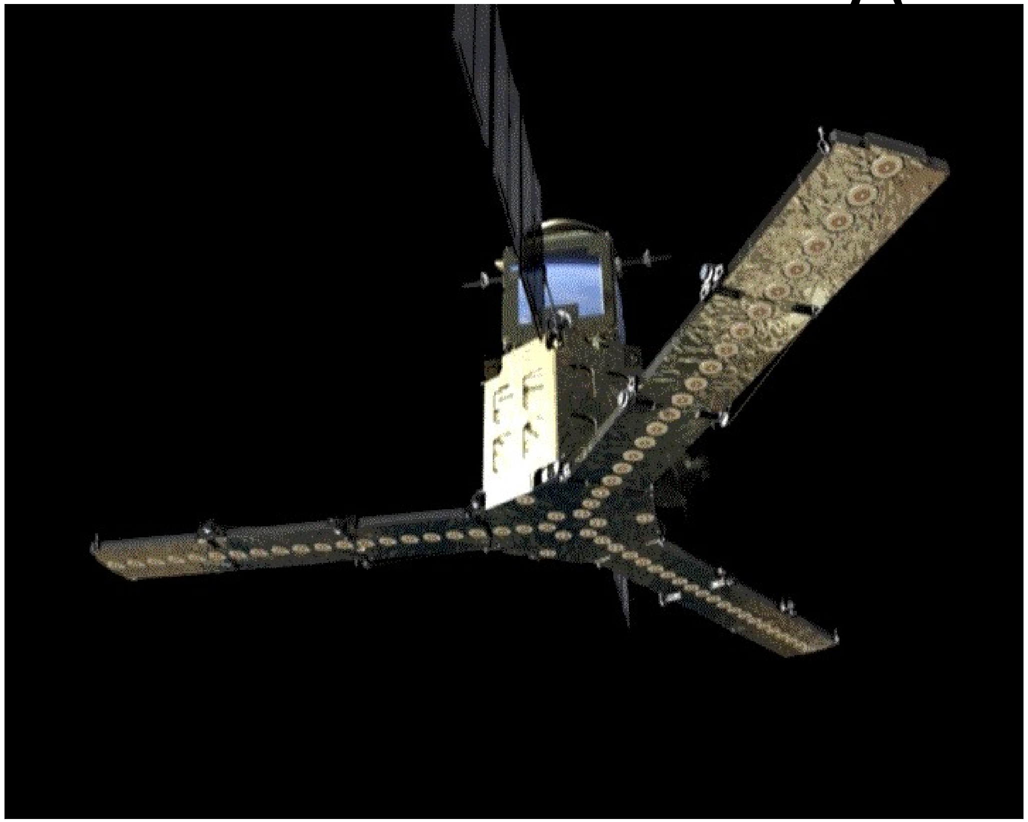

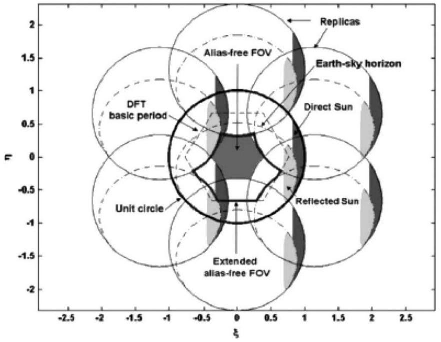

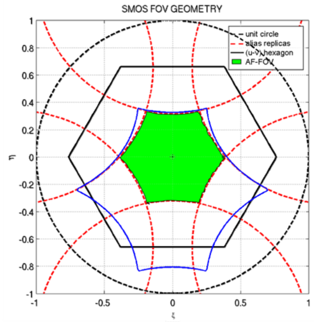

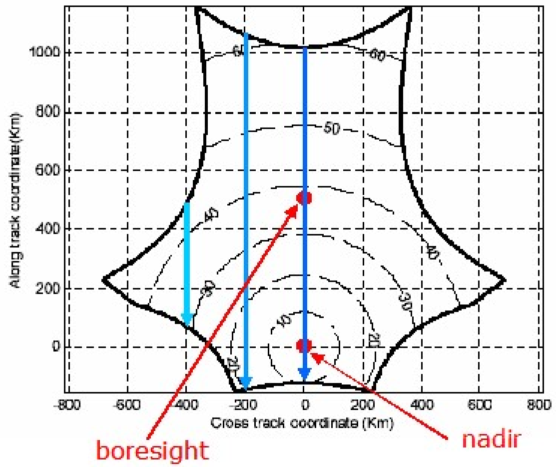

MICROWAVE RADIOMETERS

BEC SMOS SSS Products

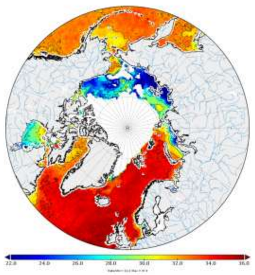

Arctic+ v3.1

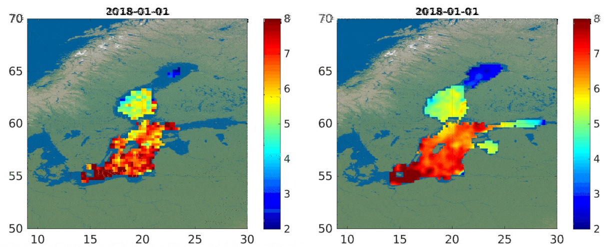

Baltic v1.0

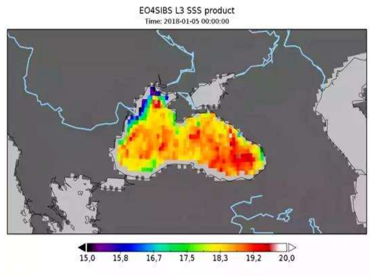

Black sea v1.0

Products accessible through BEC FTP service ***becftp.icm.csic.es***

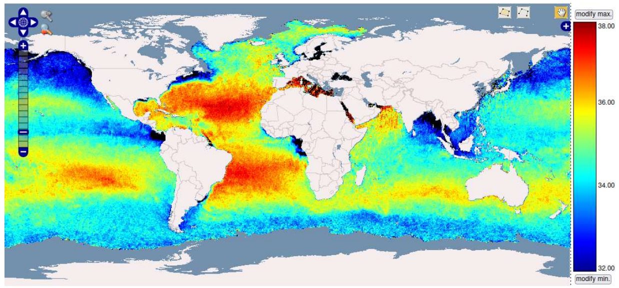

Global v2.0

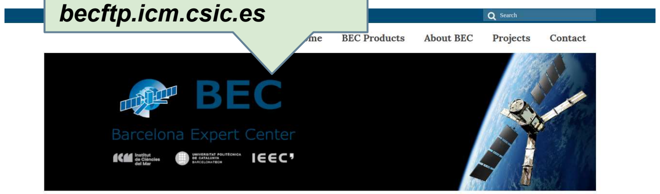

Coming soon: New products in the Southern Ocean and Enhanced Mediterranean SSS product (v3.0) !!

MICROWAVE RADIOMETERS

BEC
Barcelona Expert Center

Sensor	Platform	Agency	Dates	Frequencies	Polarization	Products
SSM/I (Special Sensor Microwave Imager)	DMSP: F8, F10, F11, F13, F14, F15	U.S. Dept. of Defense (DoD)	Sep 1987 present	19.35 22.235 37.0 85.5	V, H; V; V, H; V, H	Wind speed Water vapor Cloud water Rain rate Sea ice
TMI (TRMM Microwave Imager)	TRMM	NASA/ JAXA	Nov 1997- 2015	10.7 19.4 21.3 37.0 85.5	V, H; V, H; H; V, H; V, H	SST Wind speed Water vapor Cloud liquid
AMSR-E AMSR-2 (Advanced Microwave Scanning Radiometer)	Aqua GCOM-W1 (Shizuku)	JAXA/ NASA JAXA	May 2002- Oct 2011 May 2012- present	6.925 10.65 18.7 23.8 36.5 89.0	V, H; V, H; V, H; V, H; V, H; V, H	SST Wind speed Atmospheric
WindSat	Coriolis	U.S. DoD	Jan 2003- present	6.8 10.7 18.7 23.8 37.0	V, H; FP; FP; V, H; FP	SST, wind speed and direction
MIRAS (Microwave Imaging Radiometer with Aperture Synthesis)	SMOS (Soil Moisture and Ocean Salinity)	ESA	Jan 2009- present	1.4	V, H	SSS
Aquarius	SAC-D (Soil Moisture Active Passive)	CONAE/NASA	Jan 2011- 2015	1.41	V, H, U	SSS
GMI Microwave Imager	GMI (Global Precipitation Measurement)	NASA	Feb 2014 - present	10.65, 18,7, 23,8, 36.5, 89.0, 165.5	V,H; V,H; V; V,H;, V,H; V,H;	SST, Wind speed Water vapor Cloud water Rain rate Sea ice
Radiometer	SMAP (Soil Moisture Active	NASA	Jan 2015- present	1.41	V, H, U	SSS

ALTIMETER RADIOMETERS

BEC
Barcelona Expert Center

- Altimeters are nadir-looking radars that measure travel time and backscatter providing measures of sea level and sea state
- Measurements are constrained to satellite tracks

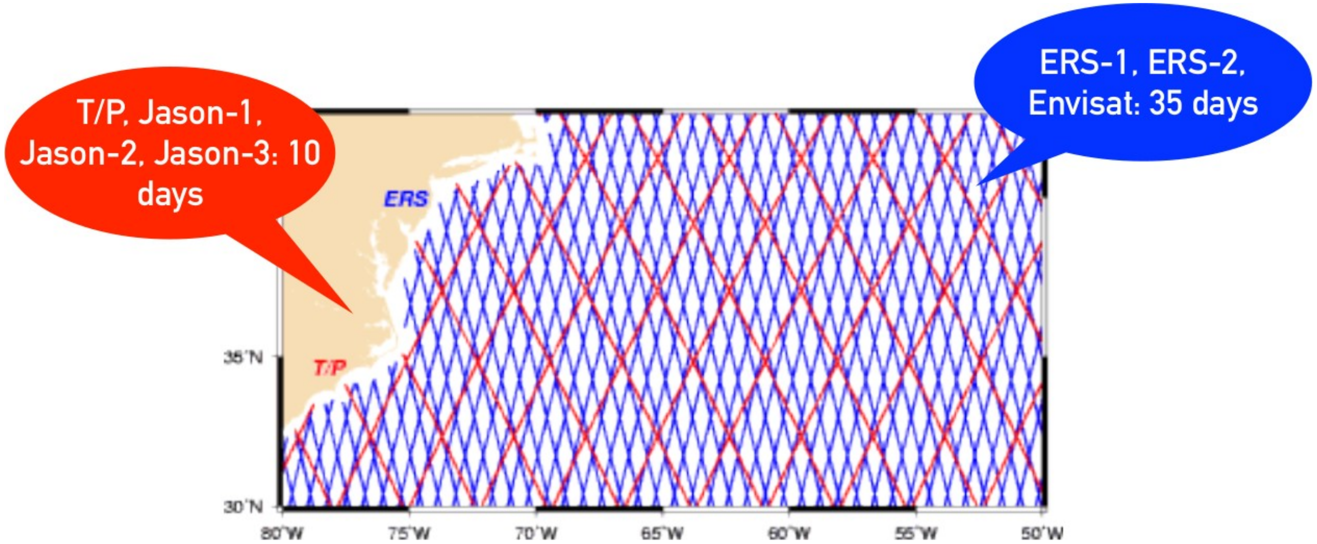

ALTIMETER RADIOMETERS

- Echo waveform has a characteristic shape that can be described analytically (the Brown model).
  - τ epoch at mid-height: range
  - P the amplitude of the useful signal: backscatter coefficient σ_0
  - P_0 thermal noise
  - leading edge slope: SWH
  - skewness: the leading edge curvature
  - trailing edge slope: deviation from nadir of the radar pointing

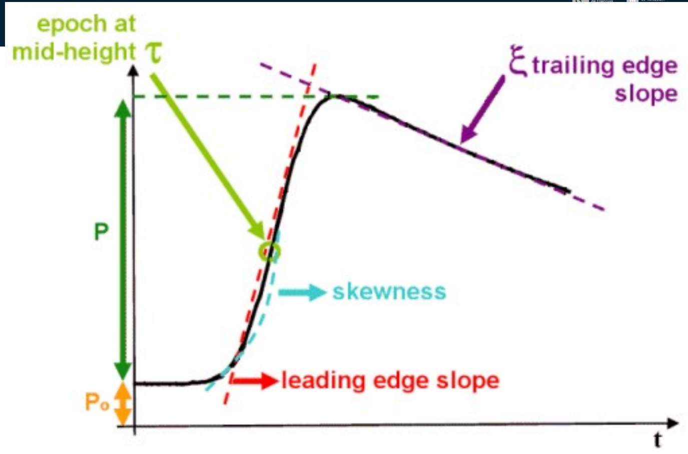

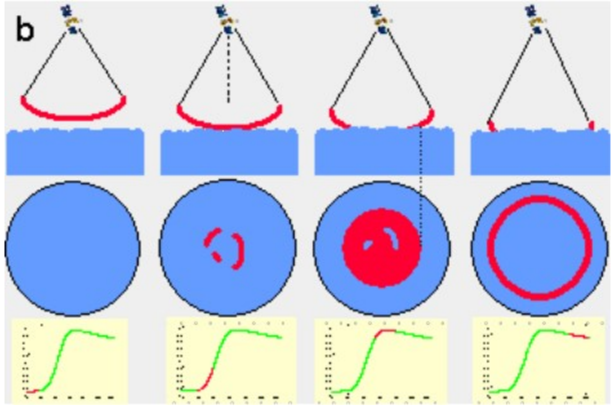

ALTIMETER RADIOMETERS

BEC
Barcelona Expert Center

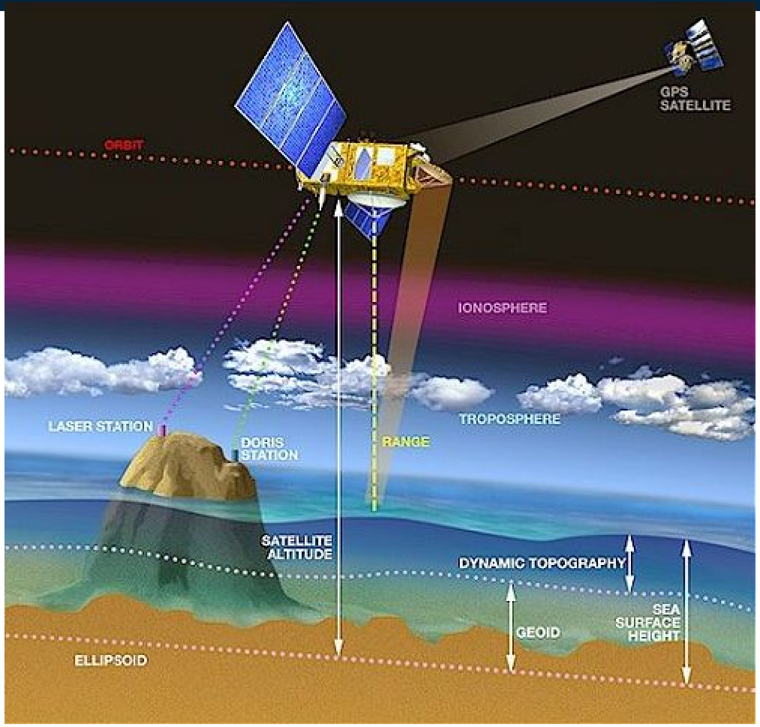

- Sea Surface Height (SSH)

$$h_{raw} = h_{sat} - R$$

- Measured SSH has several contributions

$$h_{raw} = \eta + G + h_{tide} + h_{atm}$$

- Need to apply oceanic corrections (h_{tide} , h_{atm})

- Dynamic topography η is related to currents but geoid undulations are not well known

$$h = \eta + G$$

ALTIMETER RADIOMETERS

- Geoid undulations are constant in time: Sea Level Anomalies

$$\eta' = h - \langle h \rangle$$

- Mean Dynamic Topography (MDT) determined from altimetry, gravimetric data and in situ measurements

$$\eta \approx h - \langle h \rangle + \eta_{MDT}$$

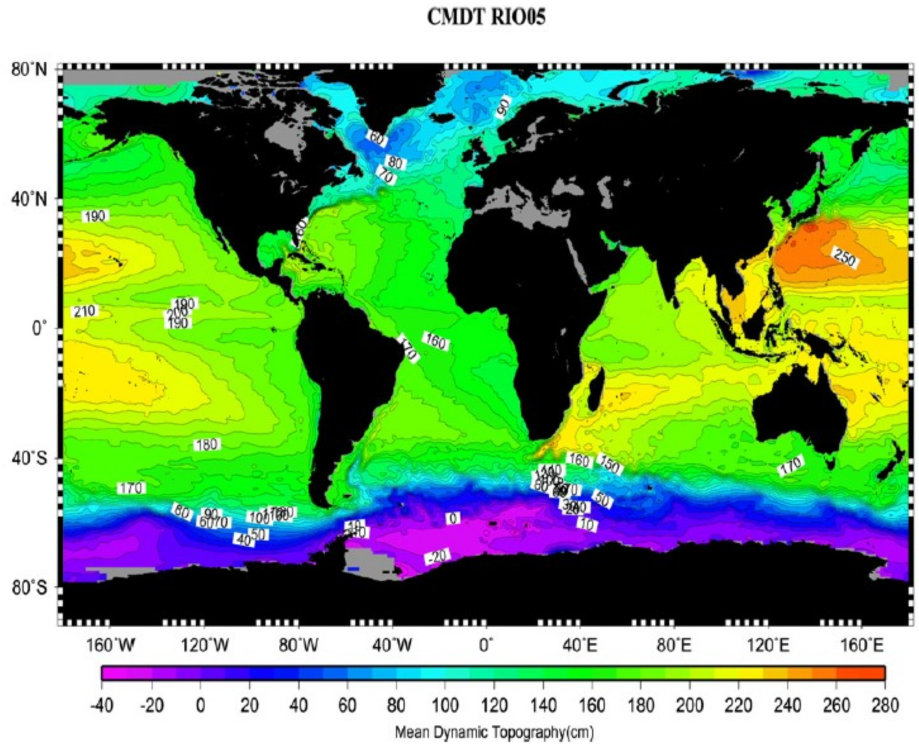

- Measurements are taken along altimetric tracks: only the cross-track velocity can be derived

ALTIMETER RADIOMETERS

- Two-dimensional fields are obtained through optical interpolation in space and time
- Basic configuration: 2 altimeters
- Shortest wavelengths ~150 km
- Error in velocities 20%-30% of variance
- Near-Real Time: past data only

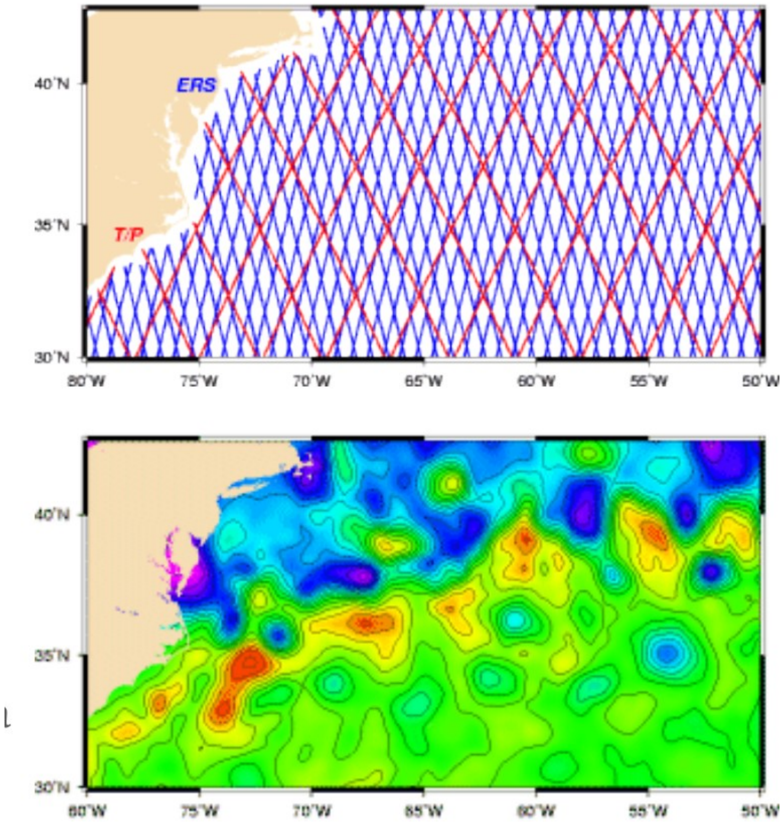

ALTIMETER RADIOMETERS

BEC
Barcelona Expert Center

Altimeter & Platform	Agency	Dates	Height	Orbit	SSHA r.m.s. accuracy
TOPEX/Poseidon	NASA/CNES	1992-2005	1 336km	9.92 day repeat non-Sun-synchronous	2-3 cm
Poseidon-2 on Jason-1	NASA/CNES	2001-present	1 336km	9.92 day repeat non-Sun-synchronous	2 cm
Poseidon-3 on Jason-2	NOAA/ NASA/CNES Eumetsat	June 2008- present	1 336km	9.92 day repeat non-Sun-synchronous	2 cm
Poseidon-3B on Jason-3	NOAA/ NASA/CNES Eumetsat	Jan 2016- present	1 336km	9.92 day repeat non-Sun-synchronous	2 cm
Radar altimeter on ERS-1	ESA	1991-2000	780km	3 & 35 day repeat Sun-	5-6 cm
RA on ERS-2	ESA	1995-2003	780km	35 day repeat Sun-synchronous	5-6 cm
RA2 on Envisat	ESA	2002-2012	800 km	35 day repeat Sun-synchronous	3 cm
Geosat	U.S. Navy	1986-1989	800km	17.05 day repeat Sun-synchronous	10 cm reanalysis
Geosat Follow-on	U.S. Navy	2000-2008	880km	17.05 day repeat Sun-synchronous	10 cm
SIRAL on Cryosat-2	ESA	2010-present	717 km	30 day repeat non Sun-synchronous	
Sentinel-3A	ESA	Jan 2016-present	814.5 km	27 day repeat non Sun-synchronous	3 cm
AltiKa on SARAL	ISRO/CNES	Feb 2013 -	800 km	35 day repeat non Sun-synchronous	
HY-2	CAST	Aug 2011 -	971 km	14 days / 168 days	

COPERNICUS PROGRAM

BEC
Barcelona Expert Center

The SENTINEL-3 mission is jointly operated by ESA and EUMETSAT to deliver operational ocean and land observation services.

The spacecraft carries four main instruments

- OLCI: Ocean and Land Colour Instrumen
- SLSTR: Sea and Land Surface Temperatu
- SRAL: SAR Radar Altimeter
- MWR: Microwave Radiometer.

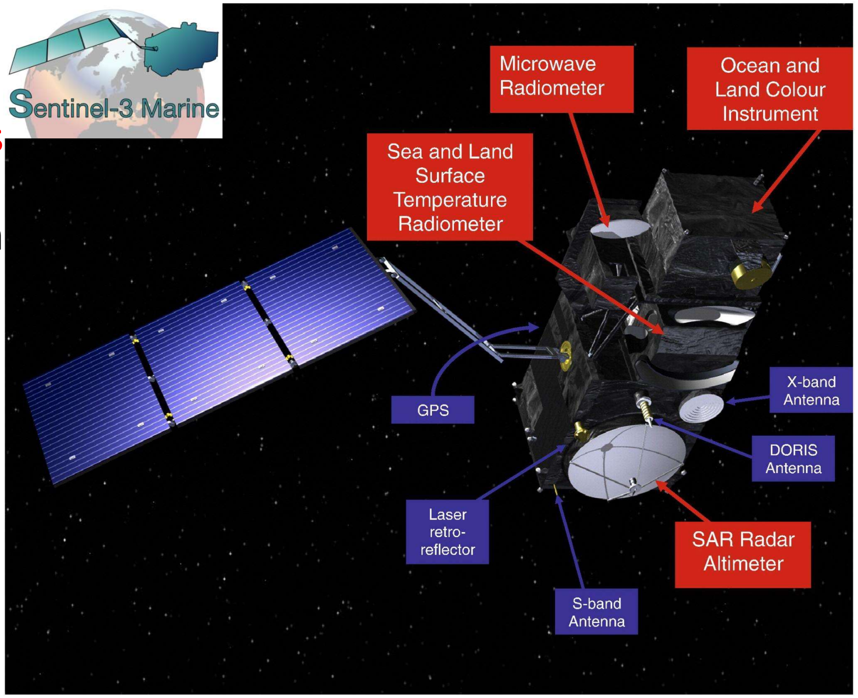

Sentinel 3: SST/SSH synergy

BEC
Barcelona Expert Center

- Simultaneous observations of SST and SSH can b… ocean surface current fields
- The reconstruction of surface currents from SST c… function (TF)

$$\hat{\psi}_s(\vec{k}) = F_T(\vec{k})e^{-i\Delta\theta(\vec{k})}\hat{T}_s(\vec{k})$$

- The TF can be derived from fluid dynamics theory
  - Surface Quasi Geostrophy (SQG) predicts that

$$\Delta\theta(\vec{k}) = 0 \qquad F_T(\vec{k}) \propto k^{-1}$$

- Our approach: to exploit the synergy between SST
  - the amplitude of SSH
  - the phase of SST

$$F_T(k) \approx \frac{g}{f_0}\frac{\langle|\hat{\eta}|\rangle_k}{\langle|\hat{T}_s|\rangle_k}$$

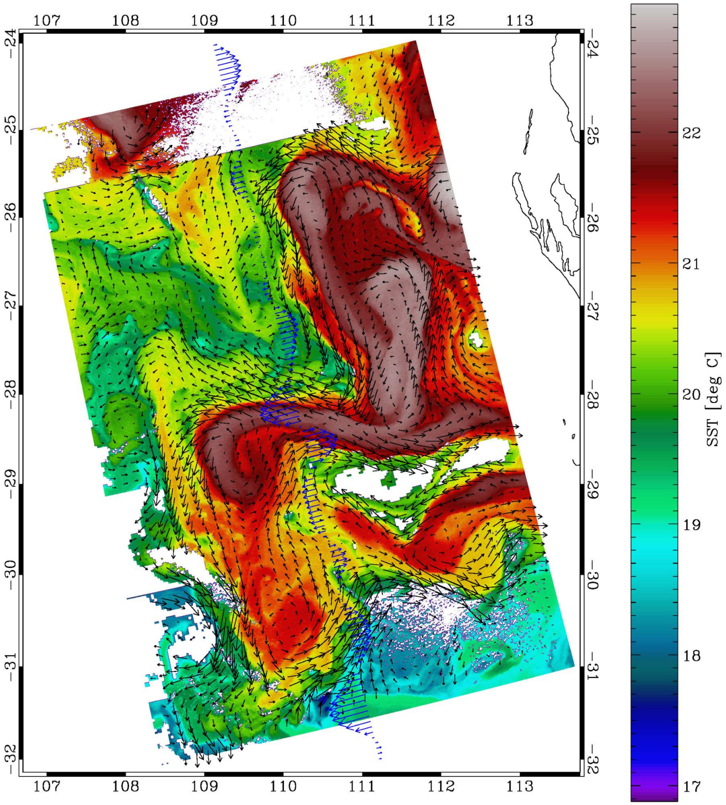

Sentinel 3: SST/SSH synergy

BEC
Barcelona Expert Center
IEEC

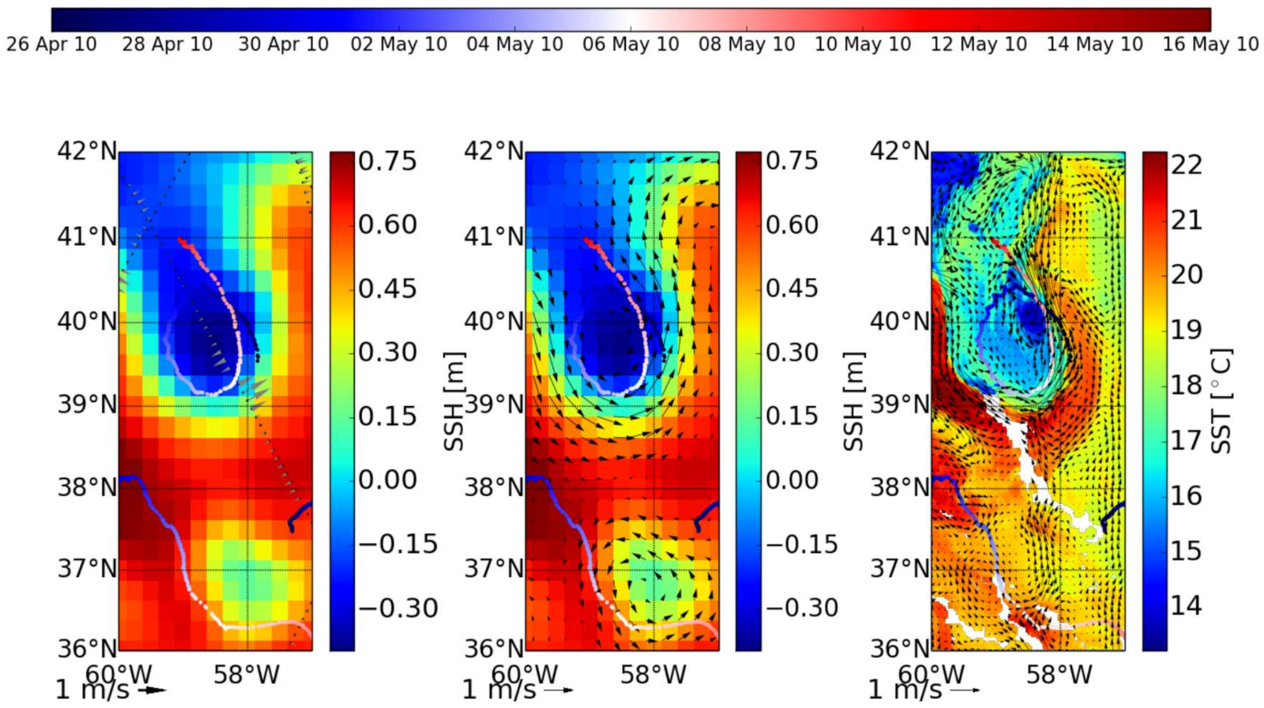

(a)

Fig. 3. left: Map of SSH gridded product corresponding on 6 May 2010 and normal component of the geostrophic velocity retrieved from all the available tracks of absolute dynamic topography (ADT), within a temporal window of 6 days centred on 6 May 2010. Middle: Map of SSH gridded product and the geostrophic velociy field retrieved. Right: Map of MODIS SST and the velocity field retrieved from it using the characterized transfer function. The horizontal color bar is common to all figures and indicates the date of the drifting buoys present in the region, which are over-plotted in every figure. It is centred on the date of SST image the 6 May 2010, blue indicates an earlier date and red later.

González-Haro et al. 2016
https://doi.org/10.1109/OCEANS.2016.7761383

Sentinel 3: accessing and visualizing

Practical training material:

https://gitlab.eumetsat.int/eur
saf-sst

https://gitlab.eumetsat.int/eur

https://gitlab.eumetsat.int/eur
case-studies/-/tree/main/

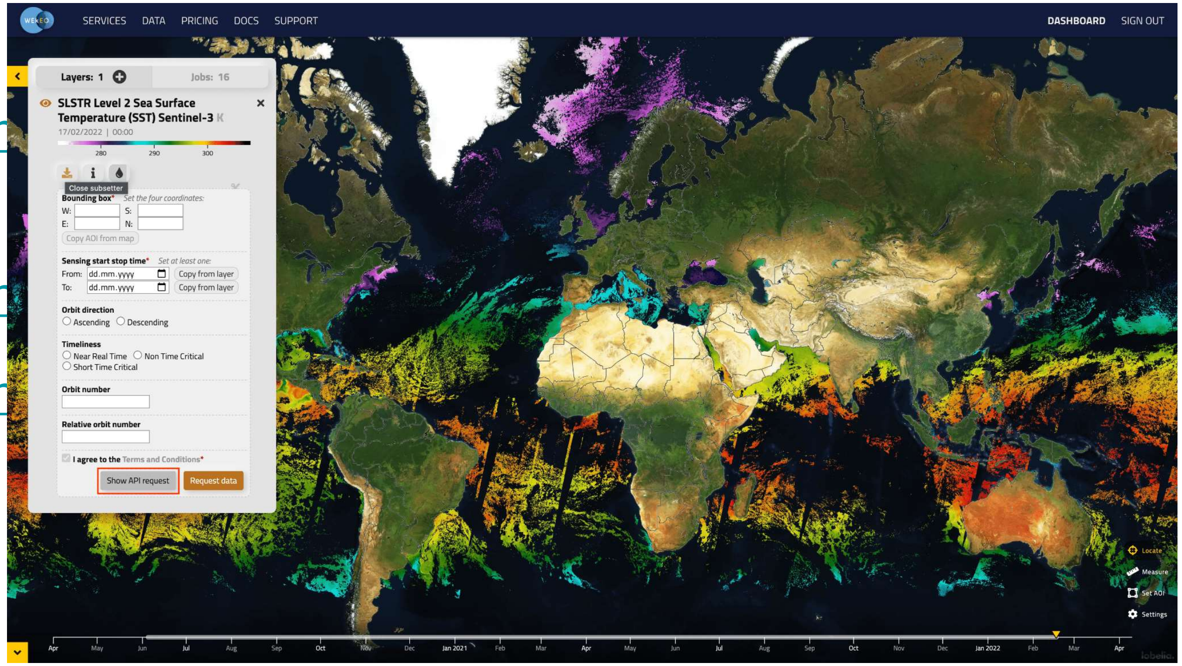

Applications: Search and Rescue

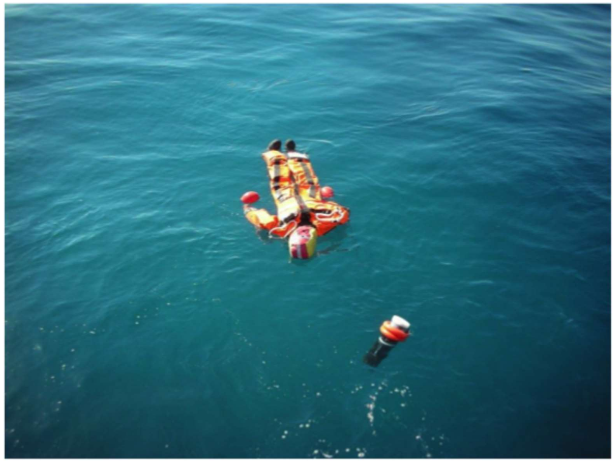

Figure 3. Image of 2 June 2015 showing the dummy with the GPS transmitter (black and orange cylinder) attached to its neck used in the Valencia experiment. Copyright SASEMAR with permission.

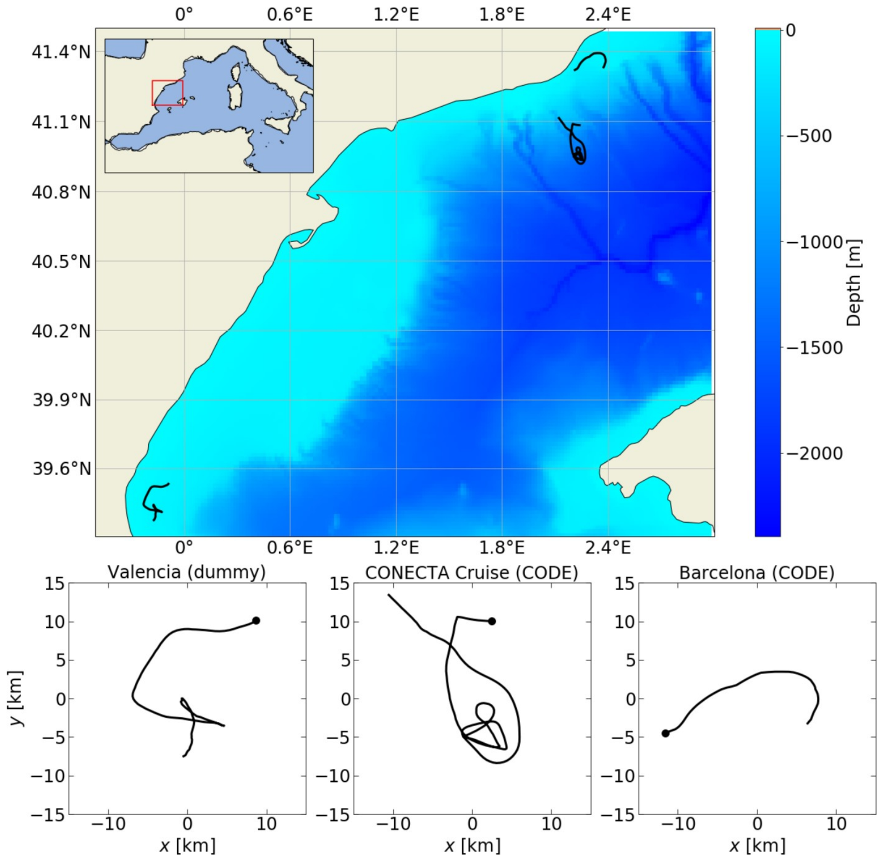

Isern-Fontanet, J., et al. (2021). High-resolution ocean currents from sea surface temperature observations: the Catalan sea (western mediterranean). Remote Sensing, 13(18), 3635.

Applications: Search and Rescue

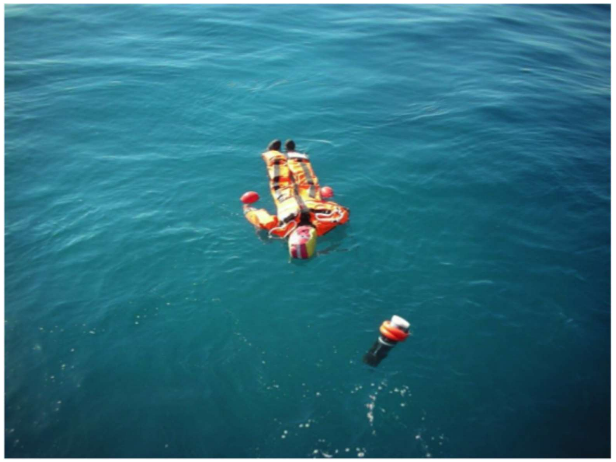

Figure 3. Image of 2 June 2015 showing the dummy with the GPS transmitter (black and orange cylinder) attached to its neck used in the Valencia experiment. Copyright SASEMAR with permission.

Isern-Fontanet, J., et al. (2021). High-resolution ocean currents from sea surface temperature observations: the Catalan sea (western mediterranean). Remote Sensing, 13(18), 3635.

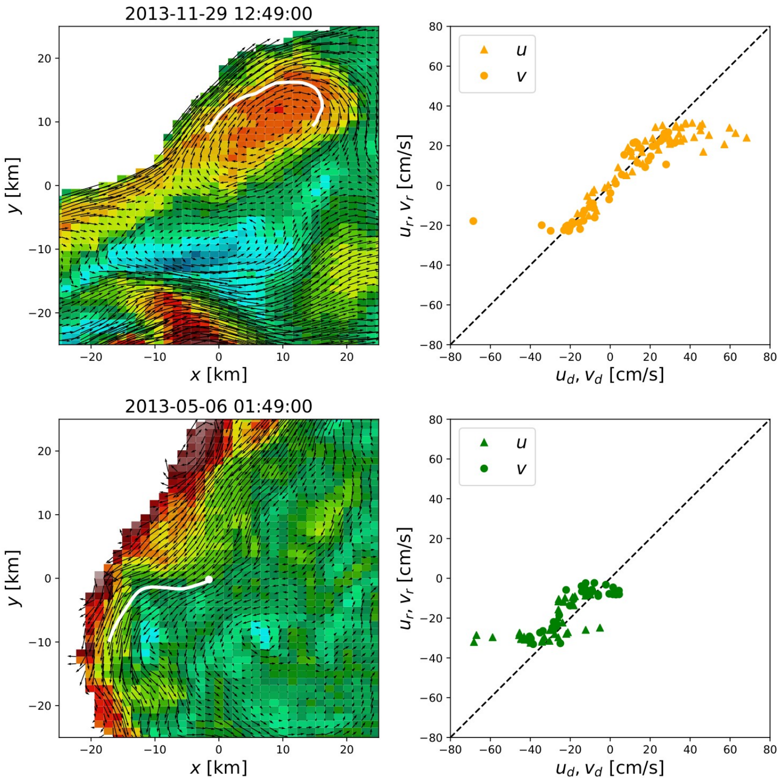

Figure 6. (**Left**) BT of coastal coherent structures with the reconstructed velocity field. White line indicated the trajectory of the drifter used for the scatter plot of the second line and the metrics shown in Table 1. (**Right**) Scatter plot between velocities derived from drifters and those obtained from the BT images. White areas correspond mainly to land areas.

REMOTE SENSING OBSERVABLE PROCESSES

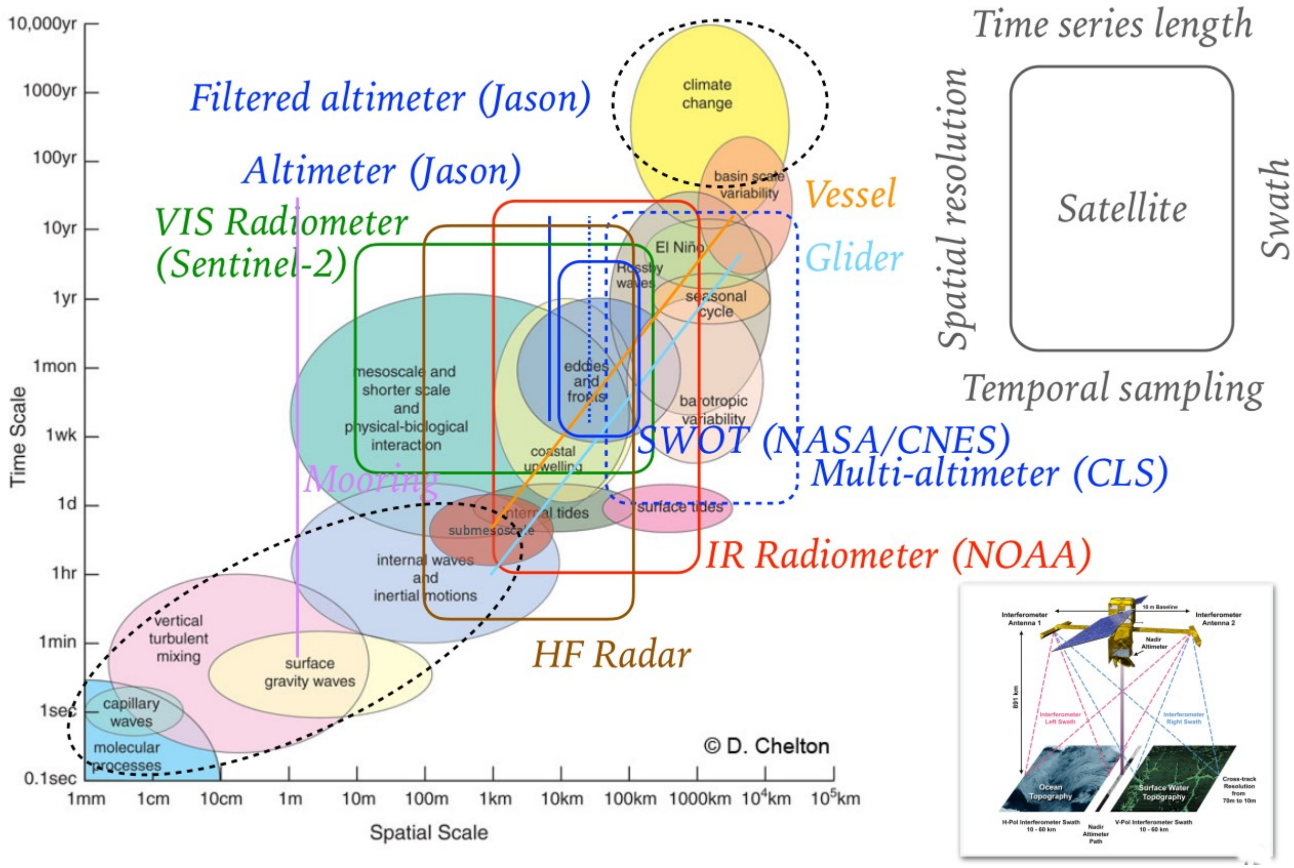

REMOTE SENSING OBSERVABLE PROCESSES

BEC
Barcelona Expert Center

Difference between size of the grid and effective spatial resolution

- The effective spatial resolution can be estimated as the spatial scale where the Power Spectrum departs from the expected power-law behaviour.

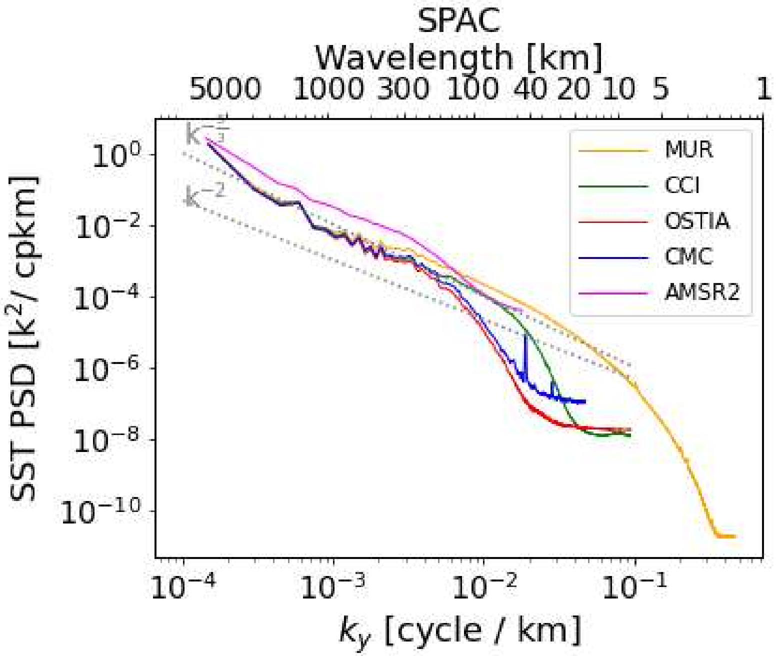

Monitorización satelital de variables esenciales climáticas: temperatura, salinidad y nivel del mar

Cristina González Haro

Institut de Ciències del Mar (ICM) - Barcelona Expert Center (BEC)

Consejo Superior Investigaciones Científicas (CSIC)

cgharo@icm.csic.es

Copernicus Satellite Data in Chile and Latin America: From applications to networking

BEC

Barcelona Expert Center

22nd March, Valparaíso, Chile

TELE DETECT